

Article

Utilization of PMA-EDTC as a Novel Macromolecular Depressant for Galena in the Flotation Separation of Chalcopyrite

Hong Zeng ^{1,2,*}, Yangge Zhu ², Chuanyao Sun ², Zhiqiang Zhao ², Guiye Wu ², Chongjun Liu ², Tong Lu ² and Xingrong Zhang ³

¹ School of Civil and Resources Engineering, University of Science and Technology Beijing, Beijing 100083, China

² State Key Laboratory of Mineral Processing Science and Technology, BGRIMM Technology Group, Beijing 102600, China

³ College of Chemical Engineering, Eco-Chemical Engineering Cooperative Innovation, Center of Shandong, Qingdao University of Science & Technology, Qingdao 266042, China

* Correspondence: zenghong@bgrimm.com

Abstract: To address the issue of mediocre separation efficiency of depressants in the copper-lead separation process, this article synthesized a macromolecular organic depressant, polymaleic anhydride-ethylenediaminetetraacetic acid (PMA-EDTC), using a polycarboxylic macromolecule as the backbone and also introducing $-N-(C=S)-S-$ as the solidophilic group and employed as a galena depressant. The structure of PMA-EDTC was characterized using Fourier transform infrared (FT-IR). The effect of PMA-EDTC on the floatability of galena and chalcopyrite was investigated through micro-flotation and Contact angle measurements. The experimental results demonstrated that PMA-EDTC exhibited selectivity inhibition towards galena rather than chalcopyrite across a wide pH range. At a dose of 8 mg/L, there was effective separation between galena and chalcopyrite with a separation coefficient of 24.17, effectively altering the floatability of galena while having little impact on the floatability of chalcopyrite. The selective inhibition behavior and adsorption mechanism of PMA-EDTC on galena and chalcopyrite were investigated using FT-IR, Zeta potential, and X-ray photoelectron spectroscopy (XPS). FT-IR and Zeta potential studies indicated that PMA-EDTC formed chemical adsorption on the surface of galena. XPS confirmed the model of chemical adsorption of PMA-EDTC on lead atoms in the galena surface. The results indicate that PMA-EDTC adsorbs on the surface of galena via its $-(C=S)-S-$ group, forming a hydrophilic complex and achieving selective depression of lead and the cleaning flotation of copper.

Keywords: galena; chalcopyrite; depressant; flotation separation; adsorption mechanism



Citation: Zeng, H.; Zhu, Y.; Sun, C.; Zhao, Z.; Wu, G.; Liu, C.; Lu, T.; Zhang, X. Utilization of PMA-EDTC as a Novel Macromolecular Depressant for Galena in the Flotation Separation of Chalcopyrite. *Minerals* **2023**, *13*, 1478. <https://doi.org/10.3390/min13121478>

Academic Editor: Andrea Gerson

Received: 20 September 2023

Revised: 20 October 2023

Accepted: 24 October 2023

Published: 24 November 2023



Copyright: © 2023 by the authors. Licensee MDPI, Basel, Switzerland. This article is an open access article distributed under the terms and conditions of the Creative Commons Attribution (CC BY) license (<https://creativecommons.org/licenses/by/4.0/>).

1. Introduction

Copper and lead are widely employed in various fields such as national defense technology, aerospace engineering, the automotive industry, construction, and electronics [1,2]. With the continuous increase in demand for copper and lead, easily exploitable rich ores are gradually depleted, leading to an increasing dependence on complex low-grade ores [1,3,4]. Concurrently, with the rapid progress of technology, driven by the requirements of new functional materials, the quality standards of copper and lead concentrate are becoming more and more stringent, which puts forward higher requirements for the flotation process and flotation reagents of complex copper and lead ore separation [5–7].

In the traditional copper-lead separation process, cyanide and its combination reagents are usually used to “reduce galena and float copper” and dichromate is used to “reduce lead and float copper”. The cyanide and potassium dichromate used are highly toxic agents [8–10]. Although these traditional inorganic inhibitors have good selectivity, their use is limited due to their high toxicity and severe environmental pollution [11–13].

Compared with the toxicity of inorganic inhibitors, small molecular organic inhibitors have the advantages of low toxicity and good selectivity. In recent years, organic inhibitors have attracted more and more attention and become a research hotspot in the field of flotation [14]. According to recent studies, the application of DPS, pseudo glycolthiourea acid, disodium carboxymethyltrithiocarbonate, thioglycolic acid, 2,3-disulfanylbutanedioic acid [15–18] in the separation of sulfide minerals demonstrates that it can be used for flotation separation of sulfide ore. The depressing activity of new organic depressant ACS to chalcopyrite and galena has been studied via artificial mixed ore and actual ore tests. The results show that ACS can depress galena well and cannot depress chalcopyrite [19]. A small reagent, O,O-bis(2,3-dihydroxypropyl) dithiophosphate (DHDTP), was investigated as a depressant on the depression of chalcopyrite and galena when ammonium dibutyl dithiophosphate (DDTP) was used as the collector in flotation tests. The flotation tests show that DHDTP has a strong depression on galena and a slight depression on chalcopyrite in a wide pH range. The Zeta potential and adsorption measurements show that DHDTP has a stronger adsorption capacity to galena than chalcopyrite [20]. Although much effort has been focused on the research of small organic inhibitors, due to their high price or poor performance in pilot scale tests, it is still a change task to apply these compounds on a commercial scale.

Natural high molecular weight organic inhibitors such as lignin, humic acid, polysaccharides, and synthetic high molecular weight organic inhibitors such as sodium polyacrylate and polyacrylamide derivatives have also been applied and studied due to their stronger hydrophilicity and lower drug consumption [21–24]. Recent research finds that synthetic large-molecule organic depressants exhibit remarkable advantages. These advantages include a diverse array of types, varied sources of raw materials, and the capacity for tailoring functional groups and molecular weights based on specific requirements [25]. Moudgil et al. [26] found that nonionic polyacrylamide possesses a certain inhibitory effect on coal. Nonionic polyacrylamide will adsorb on the surface of coal particles and render their surface hydrophilic. Boulton et al. [27] introduced several functional groups, such as carboxyl, sulfonic acid, hydroxyl, or thiourea, onto low molecular weight polyacrylamide structures to produce various polyacrylamide derivatives with unique properties. These derivatives were then utilized as pyrite inhibitors. Zhang et al. [28] explored the inhibitory effect of hydroxamate polyacrylamide on pyrite and studied the mechanism of action of hydroxamate polyacrylamide on the surface of pyrite. Consequently, the molecular design and modification of large-molecule organic depressants offer opportunities for enhancing their selectivity and inhibitory efficiency [29]. This has the potential to overcome the limitations of existing high molecular weight organic inhibitors, while also helping to address the environmental concerns of conventional inhibitors.

In this paper, an organic macromolecular galena inhibitor based on a polymaleic anhydride skeleton was designed, synthesized, and applied to the separation of copper and lead. The effectiveness of the developed organic macromolecular inhibitor in promoting the flotation separation of copper lead sulfide minerals was investigated through flotation experiments of single minerals and artificially mixed minerals. Zeta potential measurement, FT-IR spectroscopy, and X-ray diffraction (XRD) analysis techniques have been used to explore potential inhibition mechanisms, predict interaction models, and provide a theoretical basis for designing organic macromolecular inhibitors suitable for galena.

2. Materials and Methods

2.1. Minerals and Reagents

Galena and chalcopyrite samples with relatively high grades were procured from a mining site located in Hubei Province, China. These samples were crushed and finely ground in a ceramic ball mill. Subsequently, particle sizes ranging from $-74\ \mu\text{m}$ to $+38\ \mu\text{m}$ were dry-sieved in micro-flotation experiments. The X-ray diffraction (XRD) spectra and multielement analysis of both chalcopyrite and galena are presented in Figure 1 and Table 1, respectively.

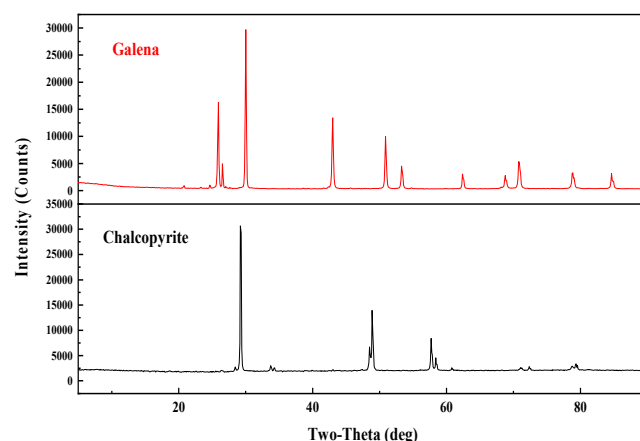


Figure 1. X-ray diffraction (XRD) results of the galena and chalcopyrite samples.

Table 1. Multi-element assay of the galena and chalcopyrite samples.

Sample	P	Zn	Pb	SiO ₂	Al ₂ O ₃	CaO	MgO	Cu	Tfe	S
Chalcopyrite	0.13	0.075	0.016	<0.01	0.040	0.11	0.078	33.95	30.84	34.54
Galena	0.0021	<0.01	84.99	<0.01	0.047	0.032	0.013	0.031	0.067	12.11

Based on X-ray diffraction (XRD) and multi-elements assay, the purity of the galena and chalcopyrite minerals sample is notably high, with galena purity at 98.14% and chalcopyrite purity at 98.23%.

The collector used in the flotation experiments, O-(2-methylpropyl) N-ethylcarbamothioate (Z-200), was sourced from BGRIMM Chemical Technology Co., Ltd. (Cangzhou, China), while the frother employed, methyl isobutyl carbinol (MIBC), was purchased from McLean Biochemical Technology Co., Ltd. (Langfang, China). Sodium hydroxide (NaOH) and hydrochloric acid (HCl), utilized as pH adjusters, were purchased from Sinopharm Chemical Reagent Co., Ltd. (Shanghai, China). The synthetic raw materials including maleic anhydride (MA), ethylenediamine, and carbon disulfide were also purchased from China National Pharmaceutical Group Chemical Reagent Co., Ltd. (Shanghai, China). All chemical reagents used above are analytical grade. Experiments were conducted in a deionized water environment.

2.2. Micro-Flotation Experiments

The micro-flotation experiments with pure minerals were conducted using a 30 mL XFGII flotation cell. Prior to micro-flotation, 2.0 g of pure mineral sample was placed into a beaker containing 30 mL of deionized water, and subjected to 5 min of ultrasonic cleaning to remove surface oxides from the minerals. After 10 min of settling, the suspension was decanted, and the bottom layer of pure minerals was transferred to the flotation cell. Subsequently, 30 mL of deionized water was added, and the required flotation reagents such as NaOH, HCl, PMA-EDTC, Z-200, and MIBC were sequentially introduced during the stirring process in the slurry. Each reagent addition was followed by a 2-min stirring period. Finally, the foam product and tailings were filtered, dried, and weighed. The recovery rates of each mineral were calculated using Formula (1). Each experiment was repeated three times to obtain an average recovery.

In the micro-flotation experiments with artificially mixed minerals, a mixture containing 1.2 g of galena and 0.8 g of chalcopyrite was used as the feed. The flotation procedure was consistent with the single mineral flotation tests. The copper and lead grades in the foam product and tailings were determined using chemical element analysis to calculate the recovery rates of copper and lead in the foam product and tailings. The copper-lead

separation coefficient in the artificially mixed mineral test was calculated using Formula (2). The flotation process diagram is presented in Figure 2.

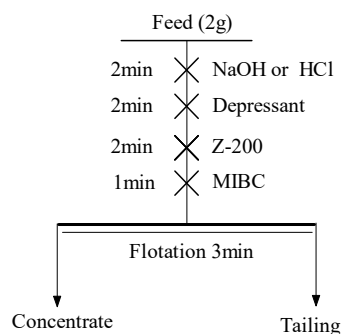


Figure 2. Micro-flotation procedure.

$$\varepsilon_s = \frac{m_c}{m_c + m_t} \times 100\% \quad (1)$$

ε_s : Recovery of valuable minerals; m_c : The mass of the concentrate; m_t : The mass of the tailings

$$I = \sqrt{\frac{\varepsilon_{11} \times \varepsilon_{22}}{\varepsilon_{12} \times \varepsilon_{21}}} \quad (2)$$

I : Separation index; ε_{11} : Recovery of valuable minerals in concentrates; ε_{12} : Recovery of gangue minerals in concentrates; ε_{21} : Recovery of valuable minerals in tailings; ε_{22} : Recovery of gangue minerals in tailings.

2.3. Contact Angle Measurements

Contact angles of liquid on mineral crystal surfaces were determined using the drop method on a Ramé-Hart 290 U4 contact angle measurement instrument (Ramé-Hart Instruments Ltd., Succasunna, NJ, USA). The contact angle measurements were conducted at room temperature using deionized water throughout the entire testing process. Polished mineral samples were placed in a 200 mL beaker, and the beaker contained 100 mL of a specified concentration of flotation reagent. The mineral samples were fully immersed in the flotation reagent solution for 20 min. After immersion, the mineral samples were removed and air-dried naturally. Subsequently, they were positioned on the sample stage of the contact angle measurement instrument for contact angle measurement. To minimize errors, each sample was measured at least three times or more.

2.4. Zeta Potential Analysis

Zeta potential was measured using a Zeta potential analyzer (Malvern Instruments Ltd., Malvern, UK). The prepared galena samples were ground to a particle size below $-5 \mu\text{m}$ using an agate mortar and pestle. Approximately 30 mg of the ground sample was weighed and placed in a beaker. Subsequently, 30 mL of potassium chloride electrolyte solution ($1.0 \times 10^{-3} \text{ mol/L}$) was added to the beaker as the electrolyte. The mixture was stirred using a magnetic stirrer for 3 min, after which sodium hydroxide or hydrochloric acid was added as a pH-adjusting agent to achieve the desired pH of the solution. Following pH adjustment, the depressant solution was added and stirred for 5 min. After the stirring process, the mixture was allowed to settle for 2 min, and the supernatant was collected for Zeta potential measurement at room temperature.

2.5. FI-IR Analysis

Fourier-transform infrared (FT-IR) spectra analysis was conducted using the pellet method on a Nicolet IS 10 (ThermoFisher, Bedford, MA, USA) Fourier-transform infrared spectrometer with a wavelength range of 4000 to 500 cm^{-1} . For the analysis, 2.0 g of

pure mineral sample was placed in a beaker containing 30 mL of deionized water. After ultrasonic cleaning, a solution of the depressant at a concentration of 1.0 g/L (30 mL) was added to the beaker. The mixture was stirred at room temperature for 30 min. The mineral sample was then thoroughly rinsed with deionized water and the resulting solid sample was vacuum-dried. The dried solid sample was subsequently subjected to FT-IR testing using the KBr pellet method.

2.6. XPS Measurements

The X-ray photoelectron spectrometer (XPS) analysis was performed using an ESCALAB 250Xi X-ray photoelectron spectrometer manufactured by ThermoFisher, USA. The analysis chamber was maintained under a vacuum pressure of 8×10^{-10} Pa, and the excitation source employed was Al K α X-ray radiation ($h\nu = 1486.6$ eV). Approximately 2.0 g of pure mineral were placed in a beaker, and an appropriate concentration of PMA–EDTC solution was added. After adjusting the pH, the mixture was stirred using a magnetic stirrer for 5 min. The physically adsorbed portion on the mineral surface was then washed off with water, followed by filtration and vacuum drying to obtain the experimental samples. Subsequently, the samples were subjected to X-ray photoelectron spectroscopy using the instrument, and the acquired data were analyzed and fitted using Avantage 5.977 software. The 284.8 eV C1s peak was used as a reference peak for calibration.

3. Results and Discussion

3.1. Synthesis and Characterization of PMA–EDTC

Preparation of Monomeric (2-aminoethyl) carbamodithioic acid (EDTC): Accurately weigh 0.1 moles of ethylenediamine and add it to a 100 mL three-neck flask. Add 60 mL of tetrahydrofuran (THF), and then cool the mixture to around 5–10 °C. Gradually add 0.1 moles of carbon disulfide within a controlled time of 30 min or less. Once the addition of carbon disulfide is complete, raise the temperature to 30 °C and continue the reaction for 2 h. Remove the THF solvent and obtain the monomeric EDTC compound through vacuum drying, with a yield of over 95%. The reaction to generate EDTC is shown in Figure 3.

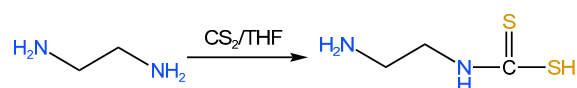


Figure 3. Synthesis route of PMA–EDTC.

Preparation of PMA–EDTC: Polymaleic anhydride (PMA) was utilized as a hydrophilic macromolecular framework, and its structure was modified through grafting with modified ethylene diamine to synthesize PMA–EDTC via a polymerization reaction. The synthesis was conducted in a water/acetone solvent system at a controlled reaction temperature of 40 °C. The synthesis process is depicted in the provided Figure 4. The molecular weight of PMA–EDTC was assessed through gel permeation chromatography (GPC), and the results are presented in Table 2.

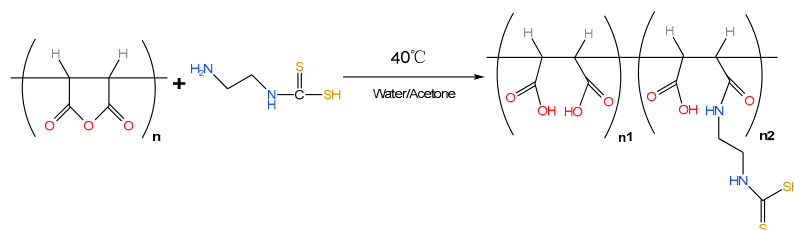
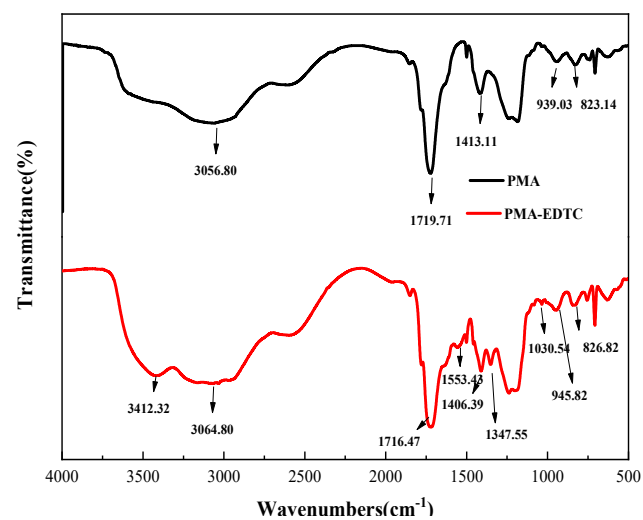


Figure 4. Polymerization of PMA–EDTC.

Table 2. PMA–EDTC gel permeation chromatography (GPC) test results.

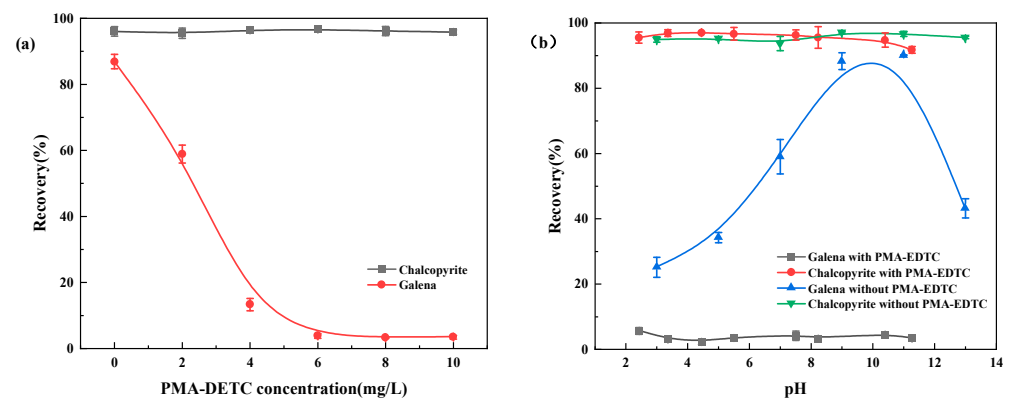
	Mp	Mn	Mw	Mz	Mz + 1	Mv	PD
PMA–EDTC	2197	1753	2067	2402	2738	2018	1.18

The FT-IR spectra of polymers PMA and PMA–EDTC are shown in Figure 5. C–H stretching vibration at 3056.80 cm^{-1} ; C=O stretching vibration at 1719.71 cm^{-1} ; C–H–O in-plane bending vibration of carboxylic acid [30] at 1413 cm^{-1} ; C–O stretching vibration at 939.03 cm^{-1} ; asymmetric stretching vibration of the epoxide ring at 823.14 cm^{-1} in the FT-IR spectrum of PMA; 1234.81 cm^{-1} is the skeleton vibration of the epoxide ring. In contrast, three new peaks appear in the IR spectra of PMA after the reaction, the peak at 1553.43 cm^{-1} is probably caused by N–H bending vibration, the peak at 1347.55 cm^{-1} is caused by C–N stretching vibration, the absorption peak at 1030.54 cm^{-1} is caused by C=S stretching vibration, the peak at 3412.32 cm^{-1} The peak at 3412.32 cm^{-1} is caused by the $-\text{NH}_2$ stretching vibration, the correctness of its structure was verified by FT-IR spectra [31].

**Figure 5.** Infrared spectra of PMA and PMA–EDTC.

3.2. Micro-Flotation Experiments

In the single mineral flotation tests, the inhibitory performance of PMA–EDTC was investigated by varying the inhibitor dosage and the slurry pH, as depicted in Figure 6.

**Figure 6.** The relationship between recovery and (a) PMA–EDTC concentration and (b) pH.

As shown in the graph, at a slurry pH around 8.5, with a frother MIBC dosage of 10.0 mg/L and a collector Z-200 dosage of 10.0 mg/L , the recovery rate of galena (lead

mineral) exhibited a rapid decline with increasing PMA–EDTC dosage, while the recovery rate of chalcopyrite (brass mineral) remained relatively stable, staying above 95%. When the PMA–EDTC dosage reached 6.0 mg/L, the recovery rate of galena dropped to 4.74%, presenting a difference of around 90% compared to chalcopyrite, underscoring the effective inhibitory role of PMA–EDTC against galena. Further increasing the PMA–EDTC dosage did not significantly alter the recovery rate of galena, thereby confirming the optimal dosage of PMA–EDTC as 6.0 mg/L.

Subsequent investigation into the influence of slurry pH on the inhibitory performance of PMA–EDTC revealed that its lead inhibitory capability remained relatively consistent across a range of slurry pH values. In the pH range of 2.0 to 12.0, PMA–EDTC consistently exhibited a strong inhibitory effect on galena while maintaining minimal impact on the floatability of chalcopyrite. Building upon the foundation of single mineral flotation experiments, additional validation of PMA–EDTC copper–lead separation efficiency was conducted through artificial mixed mineral tests.

Table 3 presents the results of artificial mixed mineral flotation experiments under various PMA–EDTC reagent dosages. The amount of trapping agent Z-200 and blowing agent MIBC was the same as in the single mineral test, and the pH of the slurry was 8.5. In the absence of the inhibitory agent PMA–EDTC, the recovery rate of Pb in the concentrate is 97.10%, while the recovery rate of Cu is 99.89%. At this point, the copper–lead separation factor is 5.3. With increasing PMA–EDTC dosage, the recovery rate of galena gradually decreases, and the copper–lead separation factor increases. When the PMA–EDTC dosage reaches 8 mg/L, the recovery rate of Pb decreases to 0.56%, while the recovery rate of Cu is 76.82%. At this dosage, the copper–lead separation factor reaches 24.17. These findings indicate that under appropriate reagent dosage conditions, PMA–EDTC exhibits significant inhibitory effects on galena, making it an effective lead inhibitor for copper–lead separation.

Table 3. PMA–EDTC artificial mixed mineral test results.

PMA–EDTC Dosage/mg·L ⁻¹	Product	Grade/%		Recovery/%		Separation Index *
		Pb	Cu	Pb	Cu	
0	Concentrate	55.95	14.20	97.10	99.89	5.30
	Tailing	35.72	0.32	2.90	0.11	
	Feed	55.05	13.58	100.00	100.00	
2	Concentrate	36.39	19.04	43.56	93.90	4.46
	Tailing	80.05	2.10	56.44	6.10	
	Feed	52.57	12.76	100.00	100.00	
4	Concentrate	6.46	33.17	4.00	76.88	8.93
	Tailing	73.87	4.75	96.00	23.12	
	Feed	52.12	13.92	100.00	100.00	
6	Concentrate	3.02	33.46	1.72	76.49	13.61
	Tailing	75.66	4.52	98.28	23.51	
	Feed	53.48	13.36	100.00	100.00	
8	Concentrate	1.08	33.60	0.56	76.82	24.17
	Tailing	75.72	4.03	99.44	23.18	
	Feed	54.49	12.44	100.00	100.00	
10	Concentrate	2.16	33.18	0.40	25.48	9.22
	Tailing	61.42	11.08	99.60	74.52	
	Feed	55.35	13.35	100.00	100.00	

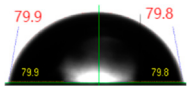
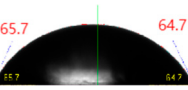
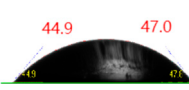
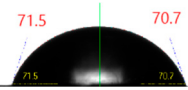
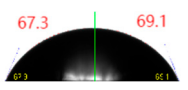
* Separation index: Indicates the degree to which a unit separation operation or a separation process separates two substances.

3.3. Contact Angle Measurements

The contact angle is a quantitative measure of surface wetting, represented by the angle formed between a liquid or vapor interface and the solid surface. In general, a larger contact angle indicates a stronger hydrophobicity of the mineral surface, suggesting better floatability. Conversely, a smaller contact angle indicates a stronger hydrophilicity of the mineral surface, implying poorer floatability [32].

The images in Table 4 illustrate the contact angle variations of galena and chalcopyrite under natural pH conditions. Upon treatment with 20.0 mg/L PMA–EDTC, the contact angle on the surface of galena decreases from 79.8° to 60.0°, while the contact angle of chalcopyrite remains relatively unchanged. As the concentration of PMA–EDTC reaches 50.0 mg/L, the contact angle on the surface of the galena further decreases to 47.1°. These results indicate that PMA–EDTC can effectively modify the floatability of galena at appropriate concentrations, with minimal impact on the floatability of chalcopyrite. These findings are consistent with the results of flotation experiments, confirming the selective inhibitory effect of PMA–EDTC on the flotation of galena while having little effect on the floatability of chalcopyrite.

Table 4. Contact angle measurement results.

Without Any Treatment (Galena)	10.0 mg/L PMA–EDTC (Galena)	20.0 mg/L PMA–EDTC (Galena)	50.0 mg/L PMA–EDTC (Galena)
			
Without Any treatment (Chalcopyrite)	10.0 mg/L PMA–EDTC (Chalcopyrite)	20.0 mg/L PMA–EDTC (Chalcopyrite)	50.0 mg/L PMA–EDTC (Chalcopyrite)
			

3.4. Zeta Potential Analysis

Flotation experiments and contact angle measurements have demonstrated the effectiveness of PMA–EDTC in reducing the floatability of galena and consequently lowering its recovery rate. To further elucidate the inhibition mechanism of PMA–EDTC on galena, we conducted Zeta potential measurements on galena before and after treatment with PMA–EDTC. The results are presented in Figure 7.

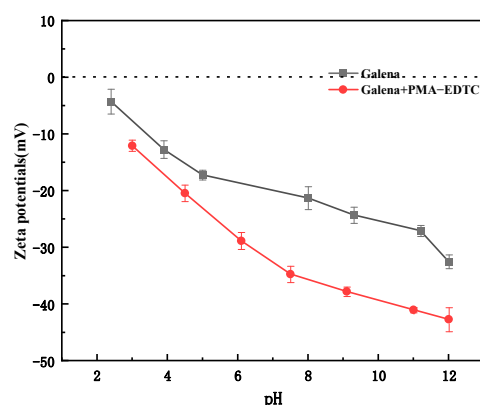


Figure 7. Effect of the pH on zeta potentials of galena before and after adding PMA-EDTC.

As depicted in Figure 7, it can be observed that the Zeta potential of galena remains consistently negative within the pH range of 2 to 12, aligning with prior reported observations. Upon the introduction of PMA–EDTC, a significant increase in the absolute value of the Zeta potential of galena is noted. This enhancement could be attributed to the presence of hydroxyl groups (–COOH) and dithiocarbamate groups (–NH–(C=S)–) within PMA–EDTC [33,34]. The chemical adsorption of PMA–EDTC onto the galena surface through its dithiocarbamate groups forms coordination complexes, while the carboxylate groups (–COO) are exposed to the aqueous phase, leading to the formation of a hydrophilic

layer on the galena surface and subsequently resulting in a decrease in the Zeta potential of galena. These outcomes collectively indicate the adsorption of PMA-EDTC onto the galena surface.

3.5. FT-IR Analysis

In order to further unravel the adsorption mechanism of PMA-EDTC on galena surface, we compared FT-IR spectra of PMA-EDTC, PMA-EDTC/Pb²⁺ complexes, and galena before and after reaction with PMA-EDTC as shown in Figure 8.

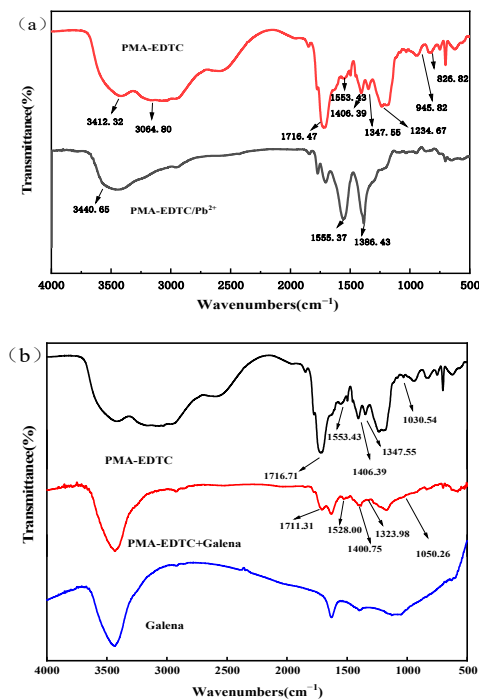


Figure 8. FT-IR spectra of (a) PMA-EDTC/Pb²⁺ complexes and (b) galena before and after PMA-EDTC treatment.

Comparing the FT-IR spectrum of the PMA-EDTC/Pb²⁺ complex with that of PMA-EDTC (Figure 8a), it is evident that the C=S stretching vibration around 1234.67 cm⁻¹ almost disappears in the complex spectrum. This disappearance suggests that C=S forms a metal coordination complex by interacting with Pb²⁺. The positions of the -NH₂, N-H, and C-N absorption peaks in PMA-EDTC also undergo changes upon complex formation, likely due to rearrangements in the molecular structure [35,36]. Through the FT-IR spectra results, it is evident that PMA-EDTC further confirmed that a chemical reaction had occurred between (-NH-(C=S)-) group with galena, providing direct evidence of chemisorption of PMA-EDTC on the galena surface.

After treatment with PMA-EDTC (Figure 8b), the galena shows a distinct peak at 1711.31 cm⁻¹. By comparing the infrared spectra of PMA-EDTC, it is determined that this peak is due to the stretching vibration of C=O in PMA-EDTC. The peaks at 1528.00 cm⁻¹ and 1323.98 cm⁻¹ are respectively caused by the N-H bending vibration and C-N stretching vibration in PMA-EDTC. The absorption peaks at 1400.75 cm⁻¹ and 1050.26 cm⁻¹ are due to the internal stretching vibration of the carboxyl group in PMA-EDTC and the stretching vibration of C=S in -C(=S)S-, respectively. The appearance of these peaks also indicates that the adsorption behavior of PMA-EDTC occurs on the surface of the galena.

3.6. XPS Analysis

The chemical adsorption of PMA-EDTC on the galena surface, as well as its capability to form metal complexes with Pb²⁺ through reaction, has been confirmed through FT-IR

spectra and zeta potential testing. To further elucidate the interaction mechanism between PMA-EDTC and the galena surface, XPS experiments were conducted to analyze the surface characteristics of the galena before and after PMA-EDTC treatment. The XPS survey spectra of PMA-EDTC and the galena before and after treatment are presented in Figure 9, and the changes in surface concentrations of elements C, N, O, S, and Pb on galena surfaces due to PMA-EDTC treatment are summarized in Table 5. As observed from Figure 9, a newly emerged N 1s peak on the galena surface after treatment indicates the adsorption of PMA-EDTC. Notably from Table 5, the concentrations of O and C on the galena surface increase upon PMA-EDTC adsorption, while the concentrations of S and Pb decrease correspondingly. These variations are attributed to the adsorption of the inhibitor PMA-EDTC on the galena surface.

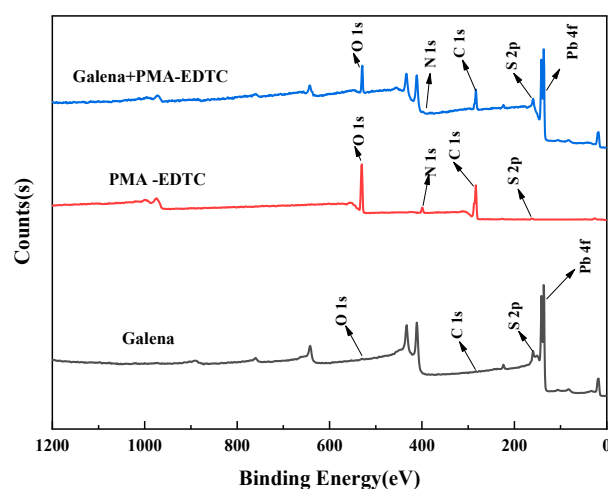


Figure 9. The wide survey scan XPS of untreated and treated galena with PMA-EDTC and PMA-EDTC complexes.

Table 5. Atomic concentration of elements with untreated and treated galena with PMA-EDTC and PMA-EDTC complexes.

Sample	Atomic Concentration of Elements (Atomic%)				
	C	O	N	S	Pb
PMA-EDTC	63.76	29.27	5.98	1.00	
Galena+PMA-EDTC	50.06	22.96	1.43	16.12	9.43
Galena	11.28	9.88		54.14	24.70
Δ a	38.78	13.08	1.43	-36.02	-15.27

To reveal the surface atomic states of the minerals, high-resolution X-ray photoelectron spectroscopy (XPS) spectra of S 2p, N 1s, O 1s, C 1s, and Pb 4f were fitted using Avantage 5.997 software, as shown in Figure 10.

The high-resolution XPS spectrum of N 1s for PMA-EDTC and PMA-EDTC treated galena is presented in Figure 10. The N 1s spectrum of PMA-EDTC can be deconvoluted into two peaks with binding energies of 400.1 eV ($-\text{CONH}_2$ or $-\text{CONH}-$) and 401.7 eV ($-\text{NH}-(\text{C}=\text{S})-$), consistent with reported values in the literature. After treatment with PMA-EDTC, two new peaks emerged at 399.5 eV and 400.4 eV on the N 1s spectrum of galena, corresponding to the ($-\text{CONH}_2$ or $-\text{CONH}-$) group and the ($-\text{NH}-(\text{C}=\text{S})-$) group within PMA-EDTC. This confirms the adsorption of PMA-EDTC onto the galena surface, with shifts of 0.6 eV and 1.3 eV observed in these two peaks. These shifts validate the alteration of the chemical environment of N atoms within PMA-EDTC due to adsorption.

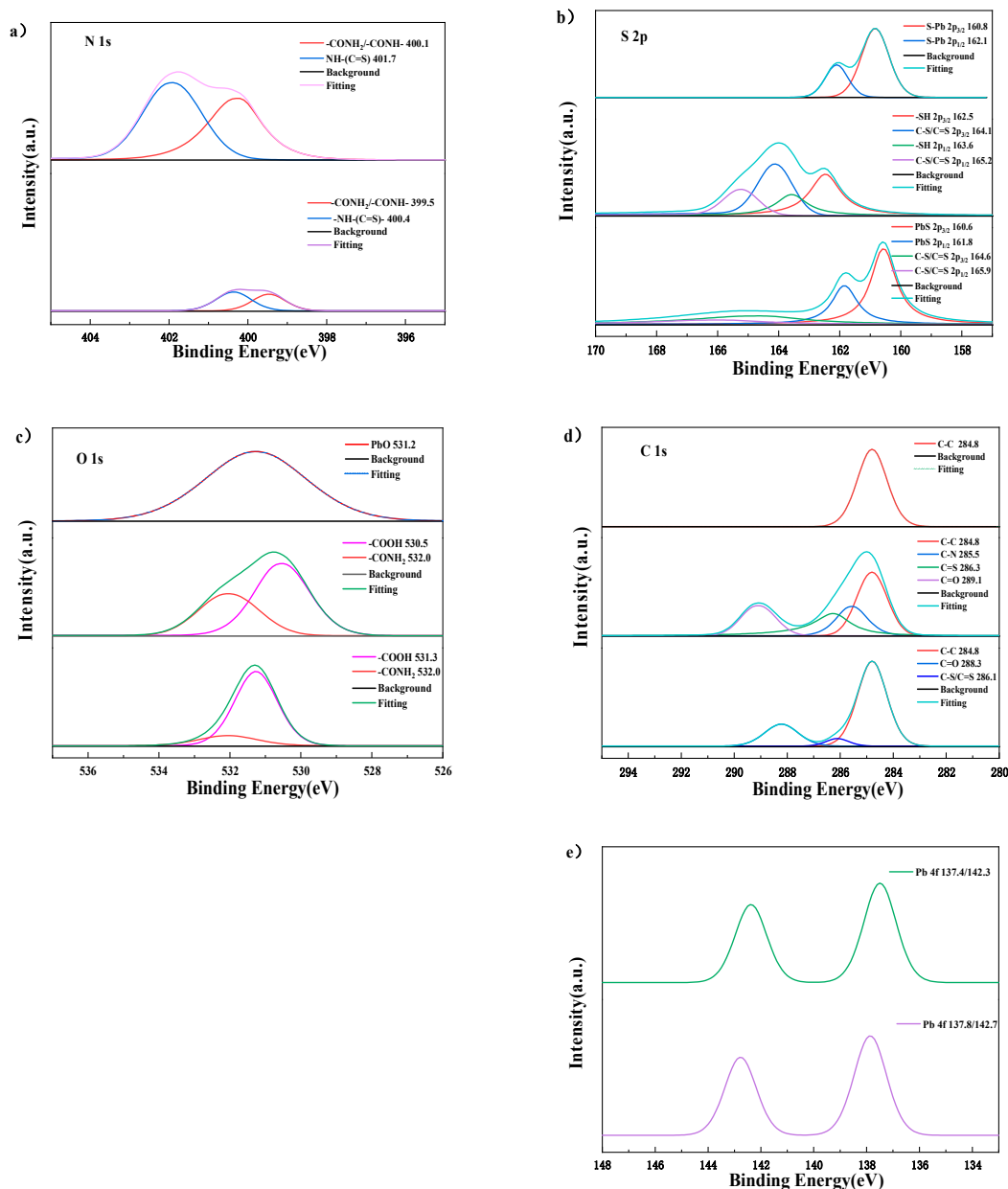


Figure 10. The fitted XPS of (a) N 1s, (b) S 2p, (c) O 1s, (d) C 1s, and (e) Pb 4f.

As depicted in the provided figure, in the high-resolution XPS spectra of S 2p for PMA-EDTC and galena, the characteristic S 2p_{3/2} peak and S 2p_{1/2} peak of pure galena appear at around 160.8 eV and 162.1 eV, respectively, with no other S 2p peaks observed. This indicates the relative purity of the galena sample [37]. Additionally, the XPS spectrum of the S 2p peak for PMA-EDTC exhibits peaks at 162.5 eV, 163.6 eV, 164.1 eV, and 165.2 eV, attributed to the (C-S/C=S) group and the (-SH) group.

After treatment with PMA-EDTC, the surface of the galena displays four S 2p peaks at approximately 160.6 eV, 161.8 eV, 164.6 eV, and 165.9 eV. The first two S 2p peaks can be attributed to the S atoms of the original galena. The latter two peaks can be assigned to the (C-S/C=S) group within PMA-EDTC, based on comparison. Hence, it can be inferred that the di-thioamino acid root group (NH-C(=S)-S) in the structure of PMA-EDTC might react with the Pb sites on the galena surface to form complexes. This confirms that the inhibitor PMA-EDTC adsorbs onto the galena surface through the di-thioamino acid root group and forms Pb-S bonds with the surface Pb sites, resulting in the inhibition effect on the galena.

The high-resolution XPS spectrum of O 1s for galena reveals a single characteristic peak fitted at 531.2 eV, which can be attributed to potential surface oxidation. In contrast, the high-resolution O 1s XPS spectrum of PMA-EDTC displays two distinct peaks, positioned at 530.5 eV (–COOH) and 532.0 eV (–CONH₂), closely aligning with previously reported values [37]. Following the adsorption of PMA-EDTC onto the galena surface, the O 1s XPS high-resolution spectrum of galena shows two peaks appearing at approximately 531.3 eV and 532.1 eV, corresponding to the two peaks in the high-resolution O 1s spectrum of PMA-EDTC. The peak assigned to (–CONH₂) experiences minimal displacement, indicating relatively weak interactions of the (–CONH₂) group with the galena surface.

In the C 1s spectrum of PMA-EDTC, four distinct peaks are observed. The main peak at 284.8 eV corresponds to carbon contamination, while the other three peaks at 285.5 eV, 286.3 eV, and 289.1 eV correspond to PMA-EDTC's C–N, C=S/C–S, and C=O groups, respectively [38,39]. On the other hand, the C 1s spectrum of galena displays only one peak at 284.8 eV, also attributed to carbon contamination. In comparison to the original galena, the C 1s XPS high-resolution spectrum of galena after interaction with PMA-EDTC exhibits three peaks, at 286.1 eV and 288.3 eV, which correspond to PMA-EDTC's C=O and C=S/C–S groups, respectively. The shift of the C=S peak by 0.8 eV suggests the involvement of the (NH–C(=S)–S–) group in the reaction with Pb sites on the galena surface, leading to a change in the electron density of carbon atoms. This further confirms the adsorption of PMA-EDTC onto the galena surface.

In the graph of the high-resolution Pb 4f spectrum of pristine galena, two identified peaks located at 137.4 eV and 142.3 eV correspond to the characteristic Pb 4f peaks of galena, closely matching reported data [40,41]. Following treatment with PMA-EDTC, these two peaks underwent shifts of approximately 0.4 eV and 0.6 eV, respectively. The increase in the electron density of Pb might stem from alterations in the chemical state of Pb on the galena surface. This leads to further evidence that PMA-EDTC has interacted with Pb sites on the galena surface [42].

Combining the molecular structure of PMA-EDTC with the analyses of XPS and FI-IR, it can be inferred that the functional group in PMA-EDTC reacting with Pb sites on the galena surface is the NH–C(=S)–S– group. The adsorption model is illustrated as shown in Figure 11. As mentioned above, the PMA-EDTC structure contains a substantial number of hydrophilic groups, resulting in hydrophilic characteristics on the galena surface. This arrangement serves the purpose of inhibiting galena, effectively achieving the suppression of the galena flotation.

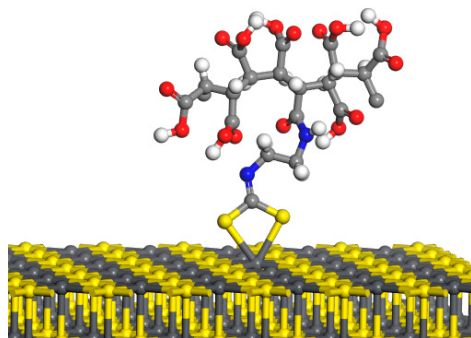


Figure 11. The recommended adsorption mode of PMA-EDTC on galena surface.

4. Conclusions

In this study, a novel macromolecular organic lead inhibitor (PMA–EDTC) was prepared by polymerizing maleic acid with NH–(C=S)–S– as a solid affinity group. The single mineral flotation test showed that PMA–EDTC had a good inhibitory effect on galena in a wide pH range of 2~12, but had little effect on the recovery of chalcopyrite. The results of the artificial ore mixing test showed that when the dosage of PMA–EDTC reaches 8 mg/L, the recovery rate of copper in the concentrate was 76.82%, while the recovery of lead was only 0.56%, and the copper-lead separation coefficient was 24.17, which further confirmed the effectiveness of PMA–EDTC as a lead inhibitor for copper-lead separation.

The FT-IR results indicated significant shifts and peak variations in the absorption peaks of the C=S–SH and –NH₂ functional groups of PMA–EDTC after interaction with Pb²⁺ ions, suggesting the occurrence of chemical reactions between PMA–EDTC and Pb²⁺ ions. Within the pH range of 2~12, treatment with PMA–EDTC resulted in a significant decrease in the Zeta potential of galena, indicating the adsorption of the reagent on the surface of galena and rendering it more hydrophilic. Contact angle measurements demonstrated that PMA–EDTC effectively altered the floatability of galena while having little impact on the floatability of chalcopyrite, achieving selective depression of lead and flotation of copper. XPS measurements further confirmed the proposed interaction model, showing that PMA–EDTC was chemically adsorbed on the lead atoms on the galena surface.

Author Contributions: Conceptualization, H.Z.; methodology, H.Z., Y.Z. and C.S.; software, C.L. and T.L.; validation, Y.Z. and Z.Z.; formal analysis, T.L. and G.W.; investigation, H.Z. and G.W.; resources, X.Z. and Z.Z.; data curation, H.Z.; writing—original draft preparation, H.Z.; writing—review and editing, G.W. and H.Z.; visualization, T.L. and G.W.; supervision, H.Z. and C.S.; project administration, C.L. and H.Z.; funding acquisition, Z.Z. and Y.Z. All authors have read and agreed to the published version of the manuscript.

Funding: This research was funded by the National Natural Science Foundation of China, grants: The interface regulation mechanism of efficient flotation separation of complicated nonferrous metal resources and the design of targeted reagent molecules (U20A20269).

Data Availability Statement: Data are contained within the article.

Conflicts of Interest: The authors declare no conflict of interest.

References

1. Cui, Y.; Jiao, F.; Qin, W.; Wang, C.; Li, X. Flotation separation of sphalerite from galena using eco-friendly and efficient depressant pullulan. *Sep. Purif. Technol.* **2022**, *295*, 121013. [[CrossRef](#)]
2. Zhang, M.; Li, J.; Li, P.; Liang, W.; Zheng, X.; Sun, K. Summarize on the lead and zinc ore resources of the world and China. *China Min. Mag.* **2016**, *25* (Suppl. S1), 41–45, 103.
3. Qin, W.; Wei, Q.; Jiao, F.; Yang, C.; Liu, R.; Wang, P.; Ke, L. Utilization of polysaccharides as depressants for the flotation separation of copper/lead concentrate. *Int. J. Min. Sci. Technol.* **2013**, *23*, 179–186. [[CrossRef](#)]
4. Cai, J.; Jia, X.; Ma, Y.; Ibrahim, A.M.; Su, C.; Yu, X.; Shen, P.; Liu, D. Effect of pre-oxidation on copper-lead bulk concentrate flotation separation with sodium polyacrylate as galena depressant. *Sep. Purif. Technol.* **2023**, *304*, 122276. [[CrossRef](#)]
5. Sehlotho, N.; Sindane, Z.; Bryson, M.; Lindvelt, L. Flowsheet development for selective Cu-Pb-Zn recovery at Rosh Pinah concentrator. *Miner. Eng.* **2018**, *122*, 10–16. [[CrossRef](#)]
6. Liu, R.; Lu, H.; Xu, Z.; Wang, C.; Sun, W.; Wu, M.; Dong, Y.; Bai, L. New insights into the reagent-removal mechanism of sodium sulfide in chalcopyrite and galena bulk flotation: A combined experimental and computational study. *J. Mater. Res. Technol.* **2020**, *9*, 5352–5363. [[CrossRef](#)]
7. Jiao, F.; Cui, Y.; Wang, D.; Hu, C. Research of the replacement of dichromate with depressants mixture in the separation of copper-lead sulfides by flotation. *Sep. Purif. Technol.* **2021**, *278*, 119330. [[CrossRef](#)]
8. Valdivieso, A.; Ledesma, L.A.; Cabrera, A.; Orozco Navarro, O.A. Carboxymethylcellulose (CMC) as PbS depressant in the processing of Pb Cu bulk concentrates. *Adsor. Float. Stud. Miner. Eng.* **2017**, *112*, 77–83. [[CrossRef](#)]
9. Huang, P.; Cao, M.; Liu, Q. Using chitosan as a selective depressant in the differential flotation of Cu–Pb sulfides. *Int. J. Miner. Process.* **2012**, *106*, 8–15. [[CrossRef](#)]
10. Pearse, M.J. An overview of the use of chemical reagents in mineral processing. *Miner. Eng.* **2005**, *18*, 139–149. [[CrossRef](#)]
11. Bulatovic, S.; Wyslouzil, D.M. Selection and evaluation of different depressants systems for flotation of complex sulphide ores. *Miner. Eng.* **1995**, *8*, 63–76. [[CrossRef](#)]

12. Zhang, X.; Lu, L.; Zeng, H.; Hu, Z.; Zhu, Y.; Han, L. A macromolecular depressant for galena and its flotation behavior in the separation from molybdenite. *Miner. Eng.* **2020**, *157*, 106576. [[CrossRef](#)]
13. Qin, W.; Wei, Q.; Jiao, F.; Li, N.; Wang, P.; Ke, L. Effect of sodium pyrophosphate on the flotation separation of chalcopyrite from galena. *Int. J. Min. Sci. Technol.* **2012**, *22*, 345–349. [[CrossRef](#)]
14. Chen, X.; Gu, G.; Chen, Z. Seaweed glue as a novel polymer depressant for the selective separation of chalcopyrite and galena. *Int. J. Miner. Metall. Mater.* **2019**, *26*, 1495–1503. [[CrossRef](#)]
15. Chen, J.; Lan, L.; Liao, X. Depression effect of pseudo glycolthiourea acid in flotation separation of copper–molybdenum. *Trans. Nonferrous Met. Soc. China* **2013**, *23*, 824–831. [[CrossRef](#)]
16. Yin, Z.; Sun, W.; Hu, Y.; Zhai, J.; Qingjun, G. Evaluation of the replacement of NaCN with depressant mixtures in the separation of copper–molybdenum sulphide ore by flotation. *Sep. Purif. Technol.* **2017**, *173*, 9–16. [[CrossRef](#)]
17. Liu, Y.; Liu, Q. Flotation separation of carbonate from sulfide minerals, II: Mechanisms of flotation depression of sulfide minerals by thioglycolic acid and citric acid. *Miner. Eng.* **2004**, *17*, 865–878. [[CrossRef](#)]
18. Li, M.; Wei, D.; Shen, Y.; Liu, W.; Gao, S.; Liang, G. Selective depression effect in flotation separation of copper–molybdenum sulfides using 2,3-disulfanylbutanedioic acid. *Trans. Nonferrous Met. Soc. China* **2015**, *25*, 3126–3132. [[CrossRef](#)]
19. Chen, J.; Feng, Q.; Lu, B. Research on a new organic depressant ASC for Separation chalcopyrite and galena. *Conserv. Util. Miner. Resour.* **2000**, *20*, 39–42. (In Chinese)
20. Piao, Z.; Wei, D.; Liu, Z.; Liu, W.; Gao, S.; Li, M. Selective depression of galena and chalcopyrite by O,O-bis(2,3-dihydroxypropyl)dithiophosphate. *Trans. Nonferrous Met. Soc. China* **2013**, *23*, 3063–3067. [[CrossRef](#)]
21. Pugh, R.J. Macromolecular organic depressants in sulphide flotation—A review, 1. Principles, types and applications. *Int. J. Miner. Process.* **1989**, *25*, 101–130. [[CrossRef](#)]
22. Kar, B.; Sahoo, H.; Rath, S.S.; Das, B. Investigations on different starches as depressants for iron ore flotation. *Miner. Eng.* **2013**, *49*, 1–6. [[CrossRef](#)]
23. Rath, R. K.; Subramanian, S. Effect of guar gum on selective separation of sphalerite from galena by flotation. *Trans. Inst. Min. Metall. Sect. C—Miner. Process. Extr. Metall.* **1999**, *108*, C1–C7.
24. De Melo, B.A.G.; Motta, F.L.; Santana, M.H.A. Humic acids: Structural properties and multiple functionalities for novel technological developments. *Mater. Sci. Eng. C* **2016**, *62*, 967–974. [[CrossRef](#)]
25. Pearse, M.J. Historical use and future development of chemicals for solid–liquid separation in the mineral processing industry. *Miner. Eng.* **2003**, *16*, 103–108. [[CrossRef](#)]
26. Moudgil, B.M. Effect of polyacrylamide and polyethylene oxide polymers on coal flotation. *Colloids Surf.* **1983**, *8*, 225–228. [[CrossRef](#)]
27. Boulton, A.; Fornasiero, D.; Ralston, J. Selective depression of pyrite with polyacrylamide polymers. *Int. J. Miner. Process.* **2001**, *61*, 13–22. [[CrossRef](#)]
28. Zhang, J.F.; Hu, Y.H.; Wang, D.Z.; Han, L. Depressant effect of hydroxamic polyacrylamide on pyrite. *J. Cent. South Univ. Technol. (Engl. Ed.)* **2004**, *128*, 6–15.
29. Bulatovic, S.M. Use of organic polymers in the flotation of polymetallic ores: A review. *Miner. Eng.* **1999**, *12*, 341–354. [[CrossRef](#)]
30. Jiménez-Hernández, L.; Estévez-Hernández, O.; Hernández-Sánchez, M.; Díaz, J.; Sánchez, M.F.; Reguera, E. 3-mercaptopropionic acid surface modification of Cu-doped ZnO nanoparticles: Their properties and peroxidase conjugation. *Colloids Surf. A Physicochem. Eng. Asp.* **2016**, *489*, 351–359. [[CrossRef](#)]
31. Yin, Z.; Hu, Y.; Sun, W.; Zhang, C.; He, J.; Xu, Z.; Zou, J.; Guan, C.; Zhang, C.H.; Guan, Q.; et al. Adsorption mechanism of 4-amino-5-mercaptopropionic acid as flotation reagent on chalcopyrite. *Langmuir* **2018**, *34*, 4071–4083. [[CrossRef](#)]
32. Huang, P.; Wang, L.; Liu, Q. Depressant function of high molecular weight polyacrylamide in the xanthate flotation of chalcopyrite and galena. *Int. J. Miner. Process.* **2014**, *128*, 6–15. [[CrossRef](#)]
33. Fullston, D.; Fornasiero, D.; Ralston, J. Zeta potential study of the oxidation of copper sulfide minerals. *Colloids Surf. A Physicochem. Eng. Asp.* **1999**, *146*, 113–121. [[CrossRef](#)]
34. Vergouw, J.M.; Difeo, A.; Xu, Z.; Finch, J. An agglomeration study of sulphide minerals using zeta-potential and settling rate. Part 1: Pyrite and galena. *Miner. Eng.* **1998**, *11*, 159–169. [[CrossRef](#)]
35. Liu, R.; Qin, W.; Fen, J.; Wang, X.; Pei, B.; Yang, Y.; Lai, C. Flotation separation of chalcopyrite from galena by sodium humate and ammonium persulfate. *Trans. Nonferrous Met. Soc. China* **2016**, *26*, 265–271. [[CrossRef](#)]
36. Lu, L.; Xiong, W.; Zhu, Y.; Zhang, X.; Zheng, Y. Depression behaviors of N-thiourea-maleamic acid and its adsorption mechanism on galena in Mo-Pb flotation separation. *Int. J. Min. Sci. Technol.* **2022**, *32*, 181–189. [[CrossRef](#)]
37. Buckley, A.N.; Woods, R. An X-ray photoelectron spectroscopic study of the oxidation of chalcopyrite. *Aust. J. Chem.* **1984**, *37*, 2403–2413. [[CrossRef](#)]
38. Yin, Z.; Sun, W.; Hu, Y.; Zhang, C.; Guan, Q.; Liu, R.; Chen, P.; Tian, M. Utilization of acetic acid-[(hydrazinylthioxomethyl)thio]-sodium as a novel selective depressant for chalcopyrite in the flotation separation of molybdenite. *Sep. Purif. Technol.* **2017**, *179*, 248–256. [[CrossRef](#)]
39. Li, W.; Li, Y. Improved understanding of chalcopyrite flotation in seawater using sodium hexametaphosphate. *Miner. Eng.* **2019**, *134*, 269–274. [[CrossRef](#)]
40. Ikumapayi, F.; Makitalo, M.; Johansson, B.; Rao, K.H. Recycling of process water in sulphide flotation: Effect of calcium and sulphate ions on flotation of galena. *Miner. Eng.* **2012**, *39*, 77–88. [[CrossRef](#)]

41. Yu, J.; Liu, R.; Wang, L.; Sun, W.; Peng, H.; Hu, Y. Selective depression mechanism of ferric chromium lignin sulfonate for chalcopyrite–galena flotation separation. *Int. J. Miner. Metall. Mater.* **2018**, *25*, 489–497. [[CrossRef](#)]
42. Wang, Y.; Xiong, W.; Zhang, X.; Lu, L.; Zhu, Y. A new synthetic polymer depressant PADEMA for Cu-Pb separation and its interfacial adsorption mechanism on galena surface. *Appl. Surf. Sci.* **2021**, *569*, 151062. [[CrossRef](#)]

Disclaimer/Publisher’s Note: The statements, opinions and data contained in all publications are solely those of the individual author(s) and contributor(s) and not of MDPI and/or the editor(s). MDPI and/or the editor(s) disclaim responsibility for any injury to people or property resulting from any ideas, methods, instructions or products referred to in the content.